Mon. Not. R. Astron. Soc. **000**, 000–000 (0000) Printed 1 February 2008 (MN LATEX style file v1.4)

Keck Imaging of the Globular Cluster Systems in the Early–type Galaxies NGC 1052 and NGC 7332

Duncan A. Forbes[1⋆], Antonis E. Georgakakis[2†], Jean P. Brodie[3‡]

[1] *Astrophysics & Supercomputing, Swinburne University, Hawthorn, VIC 3122, Australia*
[2] *School of Physics and Astronomy, University of Birmingham, Edgbaston, B15 2TT, UK*
[3] *Lick Observatory, University of California, Santa Cruz, CA 95064, USA*

1 February 2008

ABSTRACT

The presence of two globular cluster subpopulations in early–type galaxies is now the norm rather than the exception. Here we present two more examples for which the host galaxy appears to have undergone a recent merger. Using multi–colour Keck imaging of NGC 1052 and NGC 7332 we find evidence for a bimodal globular cluster colour distribution in both galaxies, with roughly equal numbers of blue and red globular clusters. The blue ones have similar colours to those in the Milky Way halo and are thus probably very old and metal–poor. If the red GC subpopulations are at least solar metallicity, then stellar population models indicate young ages. We discuss the origin of globular clusters within the framework of formation models. We conclude that recent merger events in these two galaxies have had little effect on their overall GC systems. We also derive globular cluster density profiles, global specific frequencies and in the case of NGC 1052, radial colour gradients and azimuthal distribution. In general these globular cluster properties are normal for early–type galaxies.

Key words: globular clusters: general – galaxies: individual: NGC 1052, NGC 7332 – galaxies: star clusters.

1 INTRODUCTION

Perhaps the most noteworthy of recent findings in extragalactic globular cluster (GC) research is the discovery of bimodal color distributions in the GC systems of massive elliptical galaxies. Bimodality is taken to indicate the presence of two distinct GC subpopulations.

There are at least three scenarios for producing bimodal color distributions in the GC systems of elliptical galaxies. *i)* The merger of two gas–rich (spiral) galaxies may lead to the formation of an elliptical galaxy and create an additional population of GCs in the process (Schweizer 1987, Ashman & Zepf 1992). Since the population produced in the merger formed from enriched gas it should be of higher metallicity and redder than the indigenous population. Here the expectation is that the age of the red clusters should be similar to the epoch of the merger event. Note that, according to Worthey (1994) stellar population models, this second metal–rich population will always be redder in (U–V) than the old metal–poor population if it is older than ∼1 Gyr but it will be redder in (B–I) only if it is older than ∼2 Gyr. *ii)* A multi–phase collapse (Forbes, Brodie & Grillmair 1997) can also produce a bimodal color distribution with the blue clusters forming in an early chaotic phase of galaxy formation from metal-poor gas and the red clusters forming a few Gyr later from enriched gas in the same phase that produces the bulk of the galaxy starlight. *iii)* Coté, Marzke & West (1998) describe the build-up of the GC systems of bright ellipticals via the accretion of mostly metal-poor GCs from dwarf galaxies In this third picture the red GCs are indigenous and the blue ones acquired. These three scenarios predict a different separation in age between the red and blue GCs. The merger model predicts an old population (∼age of the universe) plus a young population with the age of the merger. A multi–phase collapse also has an old population and one slightly younger (∼2–4 Gyr younger) than the other. The accretion scenario predicts that the age distribution of the blue and the red GCs will be similar unless a recent merger product has been accreted.

The key to discriminating between these possibilities

⋆ dforbes@swin.edu.au
† age@star.sr.bham.ac.uk
‡ brodie@ucolick.org

Figure 1. V-band image of NGC 1052 covering $\approx 5.6' \times 7.0'$. North is up and East is left. *Please email dforbes@swin.edu.au for a copy of this figure*

Figure 2. V-band image of NGC 7332 covering $\approx 5.6' \times 7.0'$. North is up and East is left. *Please email dforbes@swin.edu.au for a copy of this figure*

is to determine ages and metallicities for both the blue and red GC subpopulations. In principle spectroscopy is the best way to determine age and metallicity independently, however this requires very high signal-to-noise data which is rarely available for extragalactic GCs. Alternatively one can use the difference in colour of the two subpopulations, from photometry, to *constrain* the age. The latter method has only been applied to a small number of galaxies (Whitmore et al. 1997; Puzia et al. 1999; Brown *et al.* 2000; Georgakakis et al. 2000).

Here we present data from the same Keck observing run as Georgakakis et al. (2000) for two additional galaxies – NGC 1052 and NGC 7332. Both galaxies reveal signs of a recent merger or interaction, and are therefore ideal candidates to search for young GCs. Details of the data reduction, GC selection process and contamination issues can be found in the initial paper (on the young elliptical galaxy NGC 6702 and its two GC subpopulations).

In section 2 the observations and data reduction techniques are briefly described. Section 3 presents basic results for the host galaxies. Section 4 describes the GC selection, with results given in section 5. A discussion is given in 6. Throughout this paper we adopt $H_0 = 75\,\mathrm{km\,s^{-1}\,Mpc^{-1}}$.

2 OBSERVATIONS AND DATA REDUCTION

Broad–band imaging of NGC 1052 and NGC 7332, in the B, V and I, filters was carried out at the Keck-II telescope on 1999 August 17th, using the the Low Resolution Imaging Spectrometer (LRIS; Oke et al. 1995). The LRIS instrument, equipped with a TEK 2048×2048 CCD, is mounted on the Cassegrain focus providing a $0.215\,\mathrm{arcsec\,pixel^{-1}}$ imaging scale and a $6' \times 8'$ field–of–view. The total exposure times and seeing conditions are given in Table 1.

The data were reduced following standard procedures, using IRAF software. The reduced images were found to be flat to better than $\sim 2\%$. Photometric calibration was performed using standard stars from Landolt (1992). The photometric accuracy, estimated using these standard stars, is ± 0.02 mag in all three bands.

3 GALAXY PROPERTIES

In Figures 1 and 2 we show the B band Keck images of NGC 1052 and NGC 7332 respectively. Both images reveal numerous unresolved objects. Table 2 lists some basic properties of the galaxies.

The elliptical galaxy NGC 1052 has been modelled by fitting ellipses using the ISOPHOTE task within STSDAS (for the S0 galaxy NGC 7332 we used a median filter technique). During the ellipse fitting process the centre of the galaxy was kept fixed and a 3σ clipping algorithm was employed. Bright objects, as well as the central saturated parts of the galaxy, were masked out. The position angle (PA) and ellipticity (ϵ) were fit at each radius, until S/N constraints terminated the fitting process at low surface brightness. The ellipticity, position angle, 4th sine (S4) and 4th cosine (C4) Fourier components of the isophotal fits in the B-band are given in Figure 3. Similar profiles and trends are seen in the V and I band images.

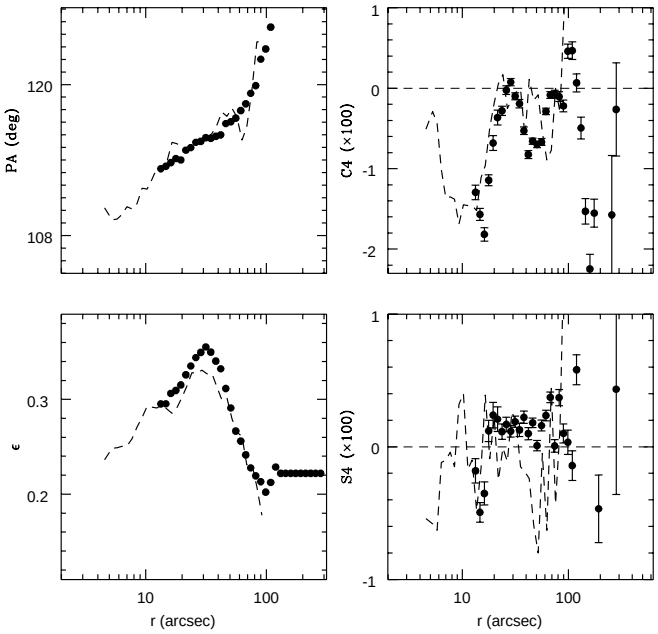

Figure 3. Radial profiles of NGC 1052 in the B-band for the ellipticity (ϵ), position angle (PA), 4th cosine term (C4) and 4th sine term (S4), estimated by fitting ellipses to the galaxy light profile. At radii larger than $\approx 130''$ both the ellipticity and the position angle are kept constant during the ellipse fitting routine, due to S/N constraints. Errors for the PA and ϵ are on the order of the symbol size. The dashed line shows the data of Peletier *et al.* (1990). The radius is the major–axis radius.

4 GLOBULAR CLUSTER SELECTION

To detect sources superimposed on the galaxies we first subtracted the galaxy light from both NGC 1052 and 7332 using a median filter and then followed the techniques described in Georgakakis et al. (2000). Briefly, sources are detected using the SExtractor package (version 2.1.0; Bertin & Arnouts 1996) with a threshold of $2.5\times\sigma_{sky}$. After detecting sources in the three filters separately, they are matched to create a list of common detections. Magnitudes were calculated using $5''$ apertures plus small aperture corrections to reach the total derived magnitude.

From the list of common detections, GC candidates are then selected on the basis of colour. In a similar way to Georgakakis et al. (2000), only those objects that fall within a region in colour–colour space corresponding to Galactic GCs but extended to higher metallicity. In particular, objects must lie between $1.2 < B - I < 2.5$ and

Name	B (secs)	V (secs)	I (secs)	Seeing (arcsec)
NGC 1052	2400	1200	300	0.8
NGC 7332	3600	1800	1200	0.8

Table 1. Observations. The total exposure time and average seeing conditions are given.

Name	Type (RC3)	A_B (mag)	Distance (Mpc)	M_B (mag)	B–V (mag)	B_{TO} (mag)
NGC 1052	E4	0.114	17.70	–19.27	0.97	24.74
NGC 7332	S0pec	0.161	15.28	–19.06	0.88	24.42

Table 2. Galaxy properties. The extinction A_B comes from Schlegel et al. (1998), the distance includes a Virgocentric infall correction for $H_0 = 75\,\mathrm{km\,s^{-1}\,Mpc^{-1}}$, M_B is the total B band luminosity of the galaxy from RC3, and B_{TO} is the expected turnover in the globular cluster luminosity function.

$0.6 < V - I < 1.7$ within 3σ photometric error. Based on colour selection alone, we find 513 and 215 GC candidates in NGC 1052 and NGC 7332 respectively. After colour selection, we automatically removed resolved objects based on their V-band FWHM size. A final visual check was then conducted.

Completeness tests were carried out by adding artificial point sources of different magnitudes to the original image, using MKOBJECTS task which are then recovered using SExtractor. The 80% completeness limits for NGC 1052 are found to be B $\approx$ 26.1, V $\approx$ 25.6 and I $\approx$ 23.6 mag. For NGC 7332 the corresponding limits are be B $\approx$ 26.8, V $\approx$ 25.7 and I $\approx$ 24.0 mag. The mean photometric error at these magnitude limits is about $\approx$ 0.1 mag for all three filters. The galaxy background does not significantly affect the completeness limits beyond a galactocentric radius of $\sim 65''$. It should be noted that including GCs brighter than the 50% completeness limit for point sources does not change any of our conclusions.

The bright magnitude is set to be about 1 mag. brighter than Omega Cen (the brightest GC in our Galaxy) at the distance of the galaxy. Sources brighter than this are most likely stars. Our magnitude limits are thus $21.0 < \mathrm{B} < 26.1$, $20 < \mathrm{V} < 25.6$, $19 < \mathrm{I} < 23.6$ for NGC 1052, and $21.5 < \mathrm{B} < 26.8$, $20.5 < \mathrm{V} < 25.7$, $19.5 < \mathrm{I} < 24.0$ for NGC 7332. After these various selection cuts we have 359 GC candidates in NGC 1052 and 154 in NGC 7332. The colour–magnitude distribution of the samples is displayed in Figures 4 and 5. Lines in these plots show the colour and magnitude limits described above.

Although we attempt to minimise the fraction of foreground stars and background galaxies in the final GC sample, it is likely that a number of contaminating sources are also selected. Details of how we estimate the contamination level in our Keck images can be found in Georgakakis et al. (2000). Briefly, we used the Galaxy model developed by Bahcall & Soneira (1980) to estimate the contamination by foreground stars. After applying the same magnitude and colour selection, the Galaxy model predicts a total of about $\approx$ 10 stars in the NGC 1052 GC sample and 24 in NGC 7332.

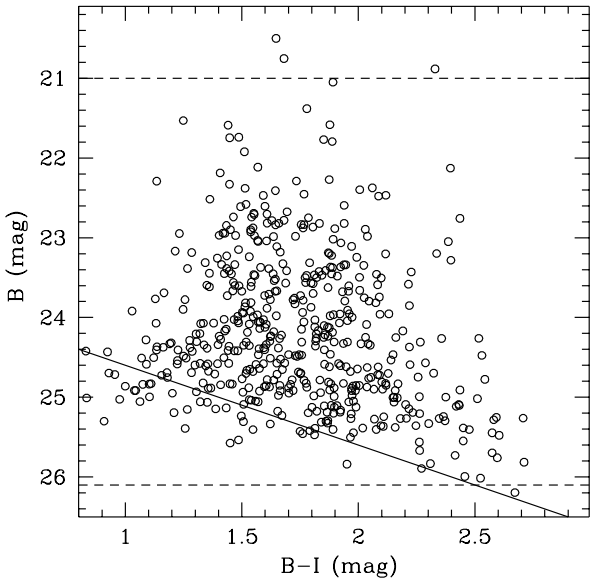

Figure 4. Colour–magnitude diagram for globular clusters in NGC 1052, after colour selection and visual inspection. The solid line corresponds to the completeness limit of $I = 23.6$ mag. The dashed lines are the B-band magnitude cutoffs for the selection of the final GC sample

Thus it both cases the number of contaminating stars in the final sample is negligible and will not effect our conclusions.

The number of background galaxies in our images are estimated from the galaxy count studies of Lilly, Cowie & Gardner (1991). From the number of predicted galaxies (within our colour and magnitude range, and field-of-view), we subtract the number of resolved objects suggesting a total of about 70 galaxies. Thus the contamination from relatively compact galaxies is estimated to be 19% for NGC 1052 and 45% for NGC 7332. Simple simulations in Georgakakis *et al.* (2000) suggest that these contamination rates are an over-

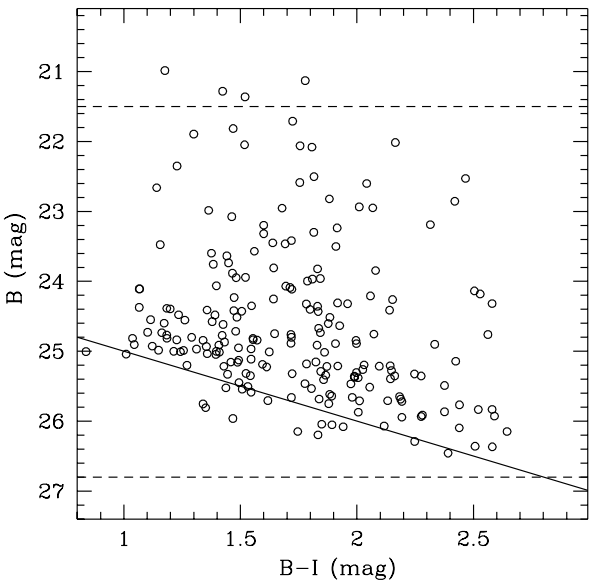

Figure 5. Colour–magnitude diagram for globular clusters in NGC 7332, after colour selection and visual inspection. The solid line corresponds to the completeness limit of $I = 24.0$ mag. The dashed lines are the B-band magnitude cutoffs for the selection of the final GC sample.

estimate and the true rate is somewhat less than this. We return to the issue of contamination in section 5.2.

5 RESULTS

5.1 NGC 1052

The colour distribution for the final NGC 1052 GC sample is plotted in Figure 6. There is evidence for bimodality with peaks in the distribution at $B - I \approx 1.5$ and $B - I \approx 1.9$. This is confirmed by the KMM statistical test (Ashman *et al.* 1994) which rejects the single Gaussian model at a confidence level better than 99.7%. Although the exact location of the peaks depend on which GCs at the extremes of the distribution are excluded, the difference in the peaks is nearly constant at around ΔB–I $= 0.4 \pm 0.1$, where the error is estimated assuming an estimated uncertainty of 0.07 mag in defining the peaks of the bimodal distribution. Also shown in Figure 6 is the reddening–corrected colour distribution of Galactic GCs. The blue peak of the NGC 1052 GCs is similar to that of the Milky Way GC distribution, which is dominated by halo GCs. The KMM test finds roughly equal numbers of blue and red GCs.

The contamination from background galaxies (i.e. 19%) is unlikely to significantly alter the results. In particular, the detection of bimodality in the NGC 1052 GC system should be robust. If we assume that the GCs comprise two distinct subpopulations of different age and metallicity but with the same initial mass function, then we can use the separation in the peak colours to constrain the age and metallicity. We further assume that the blue (older) subpopulation has properties similar to those of the Milky Way GC

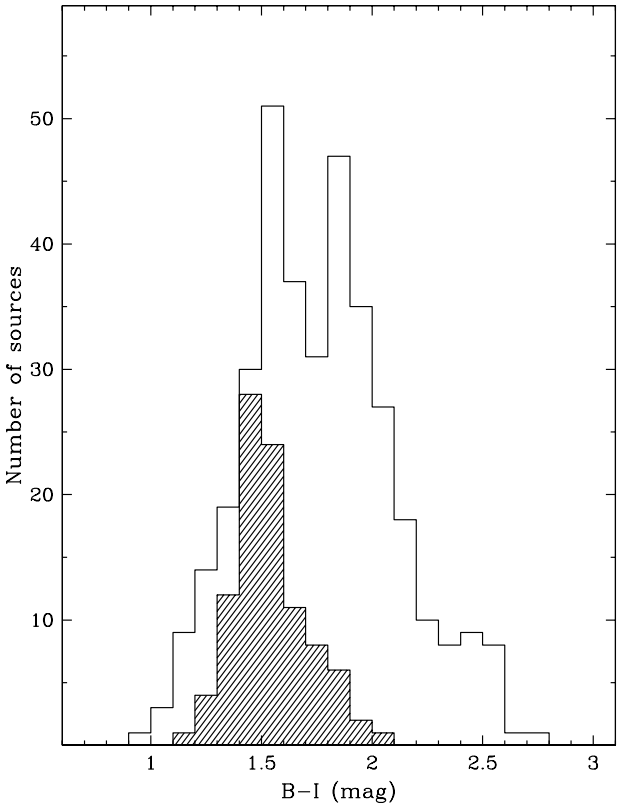

Figure 6. Colour distribution for the globular clusters in NGC 1052. Bimodality in the B–I distribution is detected at the 99.7% level from KMM statistics. Also shown is the colour distribution of Galactic globular clusters (hatched histogram). The blue peak lies close to the Milky Way globular cluster distribution (dominated by halo clusters)

system and therefore consists of old (15 Gyrs) metal–poor ([Fe/H] $= -1.5$) GCs (this is a reasonable assumption given the similarity in colour seen in Figure 6). Here we employ the models of Worthey (1994) to predict the colour difference between the red (younger) GC population and the old, metal–poor one.

The model predictions for the B–I colour difference versus age of the red subpopulation for different metallicities are shown in Figure 7. The measured colour difference in the peaks from the KMM statistical test is $\Delta(B-I) = 0.4 \pm 0.1$, where the error is estimated assuming an uncertainty of 0.07 mag in defining the peaks of the bimodal distribution.

In Figure 8 we show the trend of GC colours with galactocentric radius. The mean GC colour for the whole system appears to getter bluer with increased distance from the galaxy centre. However the mean colour of the blue ($1.1 <$ B–I < 1.7) and red ($1.7 <$ B–I < 2.3) subpopulations are fairly constant with radius. This suggests that the changing mean colour is due to a changing relative mix of red and blue GCs with radius, rather than any instrinsic radial gradient. The B–I profile for the galaxy starlight is also shown in Fig. 8. It remains fairly constant at B–I ~ 2.2.

For the same blue and red subpopulations, we have ex-

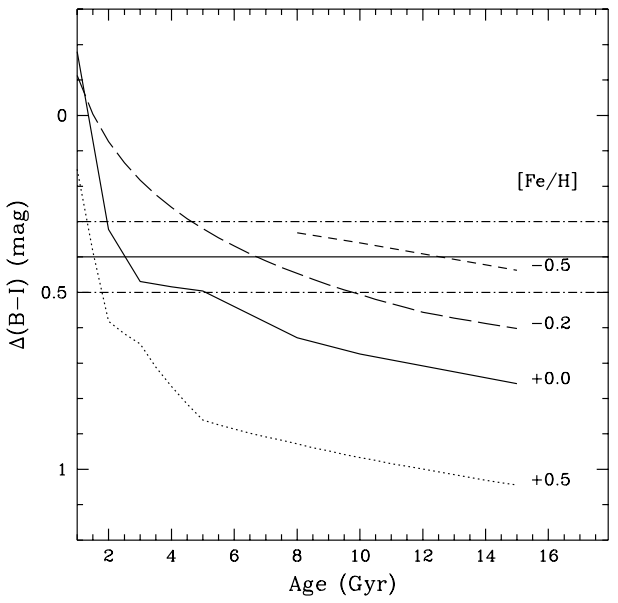

Figure 7. Colour difference versus age diagram for NGC 1052 globular clusters using the Worthey (1994) models. Each curve corresponds to a different metallicity marked on the right of the curve. $\Delta(B-I)$ is defined as the colour difference between the red and the blue (assumed 15 Gyrs old and metal–poor [Fe/H] $= -1.5$) GC subpopulations. The line corresponds to the measured colour difference in the globular cluster peaks (i.e. $\Delta(B-I) = 0.4 \pm 0.1$).

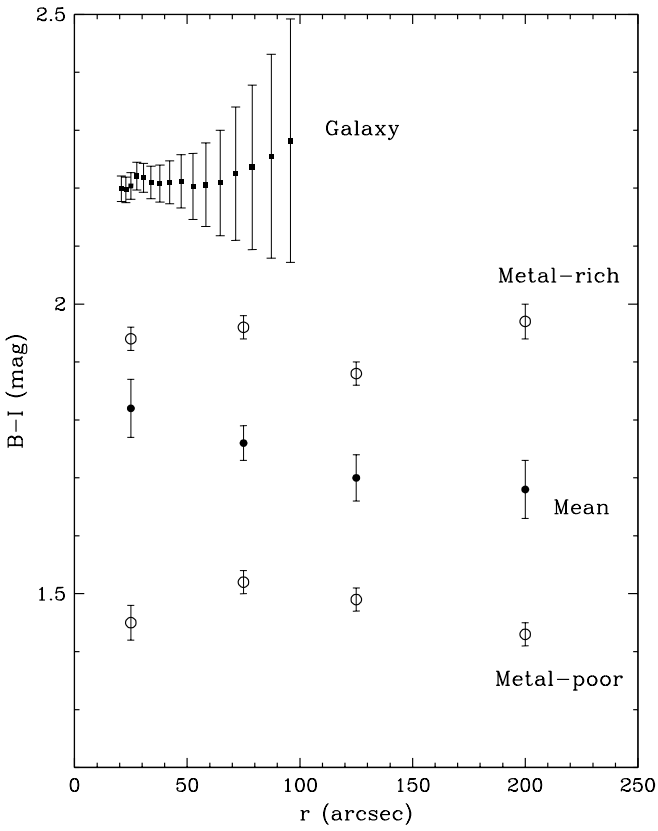

Figure 8. Radial variation of B–I colour for the globular cluster subpopulations in NGC 1052. Filled circles show the mean for the whole system, and open circles for the blue (metal–poor) and red (metal–rich) subpopulations. The mean colour (metallicity) gradient is most likely caused by a changing relative mix of the subpopulations rather than an instrinsic colour gradient. The galaxy colour profile is shown by filled squares.

amined their azimuthal distribution. In Figure 9 we show histograms of position angle for GCs within 210 arcsec. Both subpopulations show a slight tendency for the GCs to have an excess at a position angle similar to the galaxy major axis (and a deficit along the galaxy minor axis). This effect is stronger for the red GCs.

The surface density profile of GCs around NGC 1052 has been estimated in the following way. From objects detected in the V band image, we selected point sources (based on their FWHM and visual inspection) brighter than the 80% completeness limit. Using detections in a single band, instead of the colour selected GC sample, makes the selection criteria easier to quantify. These objects are then binned into elliptical rings centered on NGC 1052 and having the same mean ellipticity (i.e. 0.2) and position angle (i.e. 115°) as the galaxy. The counts in each bin are corrected for geometric incompleteness due to foreground saturated stars, bad columns and the limited size of the field–of–view (but we have not yet corrected these counts for magnitude incompleteness). The surface density profile corresponding to these counts in shown on the left of Figure 10. It is clear that the counts decline from the galaxy centre, confirming that the vast bulk of objects are indeed associated with NGC 1052. After statistically subtracting the background from the number of V band detected objects and after corrections for geometric and magnitude incompleteness (assuming V_{TO} = 23.90 and $\sigma = 1.15$), we estimate 410 ± 45 globular clusters in the LRIS frame. Integration of the surface density profile (assuming a constant density at small radii) returns a similar number of GCs, i.e. 390. We adopt 400 as the total number of GCs (i.e. covering all radii and magnitudes).

By calculating the *incompleteness* in each radial bin and assuming a standard Milky Way GC luminosity function, we correct the number counts. We also subtract a background level, which at large radii is estimated to be $\rho_{bg} = 7.23 \pm 0.05 \times 10^4$ sources deg^{-2}. The incompleteness-corrected and background-subtracted surface density profile is shown in the right side of Figure 10. A fit to the profile indicates a slope of $\alpha = -2.08 \pm 0.13$. Earlier work by Harris & Hanes (1985) found a GC surface density slope of $\alpha = -2.26 \pm 0.27$. We adopt a total GC system for NGC 1052 of 400 ± 45, this translates into a specific frequency of $S_N = 3.2 \pm 0.37$. In a previous ground-based study, Harris & Hanes (1985) estimated a total GC population of 430 ± 80 for NGC 1052. Also shown on the right hand side of Figure 10 is the normalized surface brightness profile of NGC 1052. The GC density profile shows a similar decrease with radius as the starlight.

The density profile separated into red and blue GC subpopulations is shown in Figure 11. The red GCs are slightly more centrally concentrated than the blue GCs.

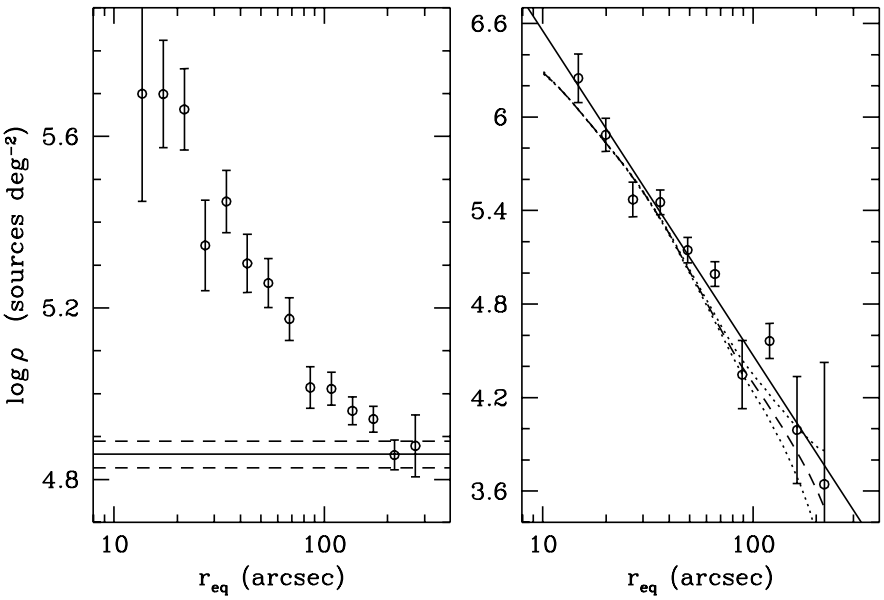

Figure 10. (a) Left panel: the surface density profile of all the objects detected in the NGC 1052 V band frame. The solid line is the mean background surface density, estimated by combining the counts in the bins at large galactocentric radii. The dashed lines are the errors around the mean assuming Poisson statistics. **(b)** Right panel: the surface density profile of the globular cluster candidates, derived by statistically subtracting the background surface density level and correcting for magnitude incompleteness. The best fit power law to the observed profile (solid line) has the form $\rho \propto r^{-2.08\pm0.13}$. The dashed line is the surface brightness profile of NGC 1052 in arbitrary units. The dotted lines represent the 1σ surface brightness uncertainty. The globular cluster distribution is more extended than the galaxy starlight.

5.2 NGC 7332

The colour distribution for the final NGC 7332 GC sample is plotted in Figure 12. There is evidence for bimodality with the peaks of the distribution at $B-I \approx 1.45$ and $B-I \approx 1.95$. After rejecting a few of the reddest objects, the KMM test rejects the single Gaussian model at a confidence level better than 97.2%, and indicates a ΔB–I = 0.5. Thus we have tentative evidence for bimodality.

Contamination by background galaxies, and to some extent foreground stars, is more of an issue for NGC 7332. For the final sample of 154 objects, we estimate that 45% may be galaxies and 15% stars. Figure 12 also shows the expected colour distribution of galaxies, superposed on that for the GC candidates. Foreground stars have a very broad colour distribution and so do not significantly modify the observed candidate GC colour distribution. Background galaxies, however, have similar colours. In particular, a significant fraction of the red peak objects are probably galaxies.

We subtract the galaxy colour distribution, and show the residual GC colour distribution in Figure 13. A narrow peak at B–I $\sim$ 1.5 remains, while the red distribution becomes much broader and less well defined. We also show in Figure 13 is the reddening–corrected colour distribution of Galactic GCs. Like NGC 1052, the blue peak of the NGC 7332 GCs is similar to that of the Milky Way GC distribution (which is dominated by halo GCs).

Given the similarity to the Milky Way colour distribution and the small number of blue galaxies, the reality of the blue GC peak seems fairly secure. However it is more difficult to be confident about the red peak. There are too few sources to investigate the red ones separately with any confidence. We proceed assuming that NGC 7332 does indeed have two GC subpopulations but any results should be regarded as tentative at best.

Following the same assumptions as above for NGC 1052, we can investigate the age and metallicity of the possible two GC subpopulations in NGC 7332. Again, relative to old (15 Gyrs), metal–poor ([Fe/H] = -1.5) GCs, the age of the red GCs can be constrained from the measured colour difference of $\Delta(B-I) = 0.5 \pm 0.14$ (we have assumed ±0.1

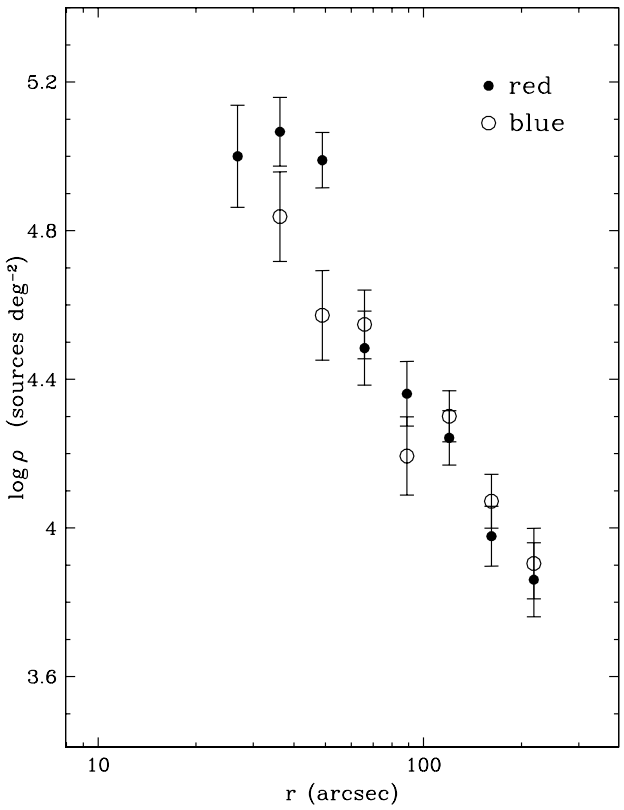

Figure 11. Globular cluster surface density of the red and blue subpopulations. The red GCs are slightly more centrally concentrated than the blue GCs.

for the individual peak colours). This color difference and the models of Worthey (1994) are shown in Figure 14.

In Figure 14 we show the surface density distribution of GC candidates around NGC 7332. This has been carried out in a similar way to NGC 1052, i.e. using the V band image we correct the counts in elliptical bins for geometric incompleteness and the limited field-of-view. These counts are converted into surface density and shown in the left panel of Figure 14. After background subtraction and correction for magnitude incompleteness, we derive the profile shown in the right panel. A fit to the final surface density profile indicates a slope $\alpha = -1.50 \pm 0.23$. The background level is estimated at $7.85 \pm 0.37 \times 10^4$ sources deg^{-2}. Subtracting this from the V band detections (after corrections for geometry, magnitude incompleteness etc) leaves 164 ± 35 objects. Integration of the surface density profile (assuming a constant density at small radii) returns a slightly higher estimate of 219 GCs. If we adopt 190 ± 30 as the total GC system, then it implies a specific frequency of $S_N = 2.0 \pm 0.3$.

We attempted to separate the density profile into the blue and red subpopulations. They show little difference, but do confirm that both subpopulations decline in density from the galaxy centre at least out to 100 arcsec. This suggests that some fraction of *both* the blue and red subpopulations are indeed associated with the galaxy. This gives us some extra confidence in the reality of the GC colour bimodality.

6 DISCUSSION

6.1 NGC 1052

Located in a small group, this E4 galaxy contains an active nucleus. Interesting features include a LINER spectrum and variable radio core (Fosbury *et al.* 1978), luminous H_2O maser (Braatz, Wilson & Henkel 1994) and an absorbed X–ray emitting nuclear source (Weaver *et al.* 1999). Although the outer stellar envelope appears to be relatively undisturbed (it has a relatively low fine structure value of $\Sigma = 1.78$; Schweizer & Seitzer 1992), it reveals multiple evidence for a past merger:

• Infalling HI gas. HI is seen in absorption redshifted on the nucleus indicating infalling HI gas (van Gorkom *et al.* 1986).
• HI tidal tails. Extended HI mapping reveals two tidal tails, indicative of a gaseous merger about 1 Gyr ago (van Gorkom *et al.* 1986).
• Misaligned star/gas axis. The rotation axis of the HI gas (PA = 134^o) and ionized gas (125-131^o) is misaligned with the stellar rotation axis (28^o). This indicates an external origin for the gas (van Gorkom *et al.* 1986).
• Dust lanes. Optical imaging (Forbes, Sparks & Macchetto 1990) indicates the presence of dust lanes near the galaxy centre. Such a structure is unlikely to arise from *in situ* stellar mass loss.

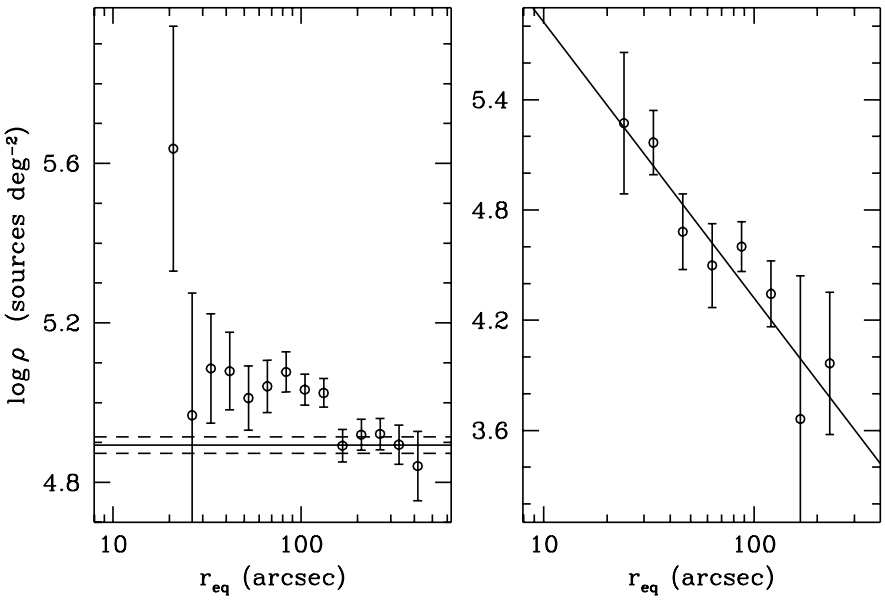

Figure 15. (a) Left panel: the surface density profile of all the objects detected in the NGC 7332 V band frame. The continuous lines is the mean background surface density, estimated by combining the counts in the bins at large galactocentric radii. The dashed lines are the errors around the mean assuming Poisson statistics. **(b)** Right panel: the surface density profile of the globular cluster candidates, derived by statistically subtracting the background surface density level and correcting for magnitude incompleteness. The best fit power law to the observed profile (continuous line) has the form $\rho \propto r^{-1.5\pm0.23}$.

Evidence for a past merger/accretion event seems overwhelming. However the time since the merger warrants further study. The HI tails would suggest a very recent merger (i.e. $\sim$ 1 Gyr), whereas the lack of optical disturbance and a Fundamental Plane residual of +0.07 (Prugniel & Simien 1996) would suggest a long time has elapsed since the last major burst of star formation (Forbes, Ponman & Brown 1998). A reliable spectroscopic age for the galaxy stars is not yet available. To be consistent with the time since the HI tails formed, the red GCs would need to have a metallicity of at least solar (for [Fe/H] $\geq$ 0, the implied age from Figure 7 is $\leq$ 2.5 Gyrs). If the red GCs were indeed this metal–rich and young, it would support arguments for their formation in the same merger event that formed the HI tails. However, GCs this young would also be expected to be brighter on average than the blue GCs, even if metal–rich (Worthey 1994). Examination of Figure 4 shows that this is not the case, i.e. the red GCs are about 0.5 mag *fainter* on average than the blue ones. The current HI content, of a few 10^8 $M_\odot$ (van Gorkom *et al.* 1986), suggests that the most recent merger will not produce significant numbers of GCs for typical gas-to-cluster formation efficiencies. So although a recent merger has occurred in NGC 1052, that event seems very unlikely to be responsible for the population of red GCs. Globular cluster formation in a very old merger, via multi–phase collapse or from accretion would appear more likely indicating that the red GCs are metal–poor, e.g. [Fe/H] $\sim$ –0.5.

The properties of NGC 1052 GC system appear to be unexceptional. We derive a specific frequency, S_N, of 3.2. This is typical for ellipticals in groups (Harris 1991). With S_N = 3.2 and a GC density profile slope of α = –2.08, the galaxy lies is within the S_N–slope trend seen by Forbes *et al.* (1997). Like other galaxies (Geisler *et al.* 1996; Forbes *et al.* 1998) the apparent radial gradient in GC mean colour appears to be due to the fact that the red (metal–rich) GCs are more centrally concentrated than the blue (metal–poor) ones. Thus the intrinsic gradient is weak. In a collapse scenario this suggests that dissipation has not played a strong role. The galaxy starlight has a similar (it is redder by about 0.25 mags) colour than the red GCs, as is often seen in other galaxies (e.g. Forbes & Forte 2000). It suggests that the red GCs and the galaxy field stars may have formed at similar times from similar enriched gas. The red, and to a lesser ex-

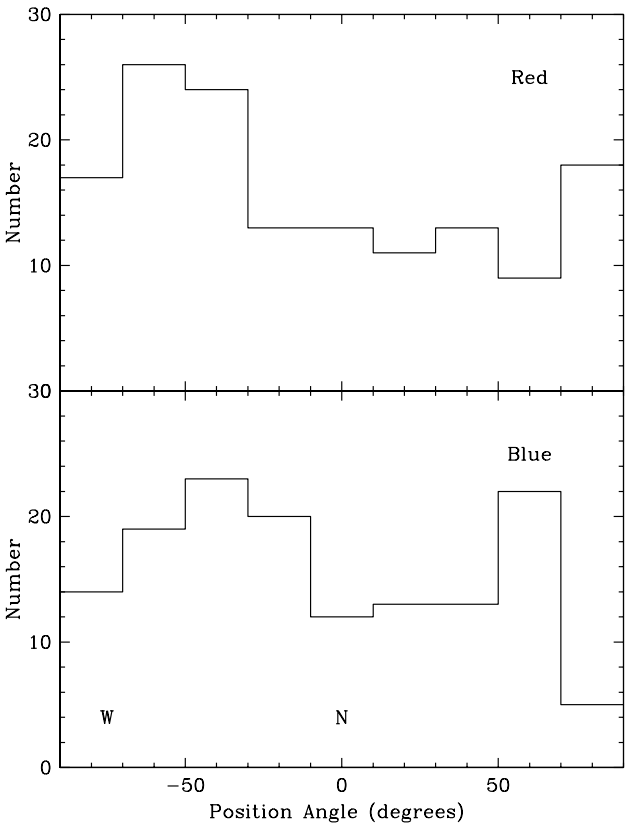

Figure 9. Azimuthal distribution of globular clusters within $210'$ of NGC 1052. The galaxy major axis is at position angle ~ 120 or -60^o. There is some evidence that the position angle of the red subpopulation is aligned with the galaxy major axis.

tent the blue, GC systems appear to be aligned in position angle with the galaxy major axis.

In terms of GC formation models, most of the GC system properties would be consistent with those expected from either an old merger (Ashman & Zepf 1992) or the multi–phase collapse (Forbes *et al.* 1997). One feature that favours the multi–phase collapse idea is the tendency for the red GCs to be more closely aligned in position angle to the galaxy starlight than the blue GCs. This is a direct consequence of the red subpopulation forming during the 'galactic' phase in which the bulk of the galaxy stars also form.

6.2 NGC 7332

This S0 galaxy reveals evidence for distortions in the outer isophotes. Schweizer & Seitzer (1992) assigned it $\Sigma = 4.00$, indicating high optical disturbance. It also lies off the Fundamental Plane by –0.31 dex (Prugniel & Simien 1996) suggesting a young age (Forbes *et al.* 1998). Indeed spectroscopy of the galaxy centre indicates an age since the last major burst of star formation of 4.5 Gyrs (Terlevich & Forbes 2000). Studies of the ionized gas reveal evidence for two components, one of which is counter–rotating with respect to the stellar distribution (Plana & Boulesteix 1996). Such

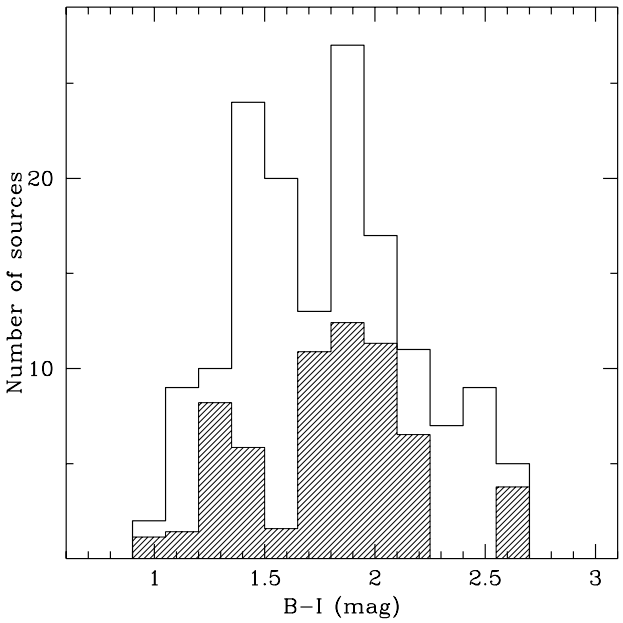

Figure 12. Colour distribution for the globular clusters in NGC 7332, and predicted distribution of contaminating galaxies (hashed histogram). See text for details.

evidence suggests that NGC 7332 is a good candidate for a recent merger event.

If the red GCs formed in a merger event less than 5 Gyrs ago, then a metallicity of at least solar is indicated by the Worthey (1994) models (see Figure 13). This would be consistent with the spectroscopic age of the galaxy, but we remind the reader of the tentative nature of the bimodal colour distribution. An old age for the red GCs (expected under the accretion and multi–phase collapse models) would require they be metal–poor, e.g. around half solar. Assuming that the red subpopulation is indeed dominated by GCs, we can not currently discriminate between GC formation in a recent merger event or *in situ* associated with the bulge/disk of the galaxy.

We derive a relatively shallow slope for the radial GC surface density of α of –1.5, and a low specific frequency S_N of 2.0, however such values remain uncertain due to the possible high contamination rate.

7 CONCLUSIONS

Here we present multi–colour Keck imaging of two nearby galaxies thought to have undergone a merger. After colour, magnitude and visual selection we detect 359 and 154 globular cluster candidates in NGC 1052 and NGC 7332 respectively. We derive globular cluster density profiles, global specific frequencies and in the case of NGC 1052, globular cluster radial colour gradients and azimuthal distribution. In general these globular cluster properties are normal for early–type galaxies.

Both galaxies also reveal a bimodal globular cluster colour distribution indicating two globular cluster subpopulations (although in the case of NGC 7332 the red subpopu-

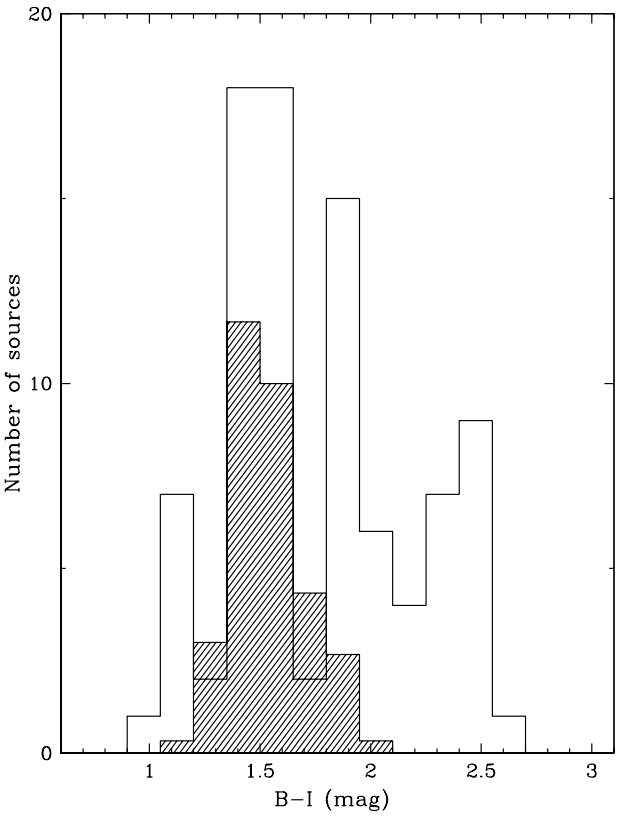

Figure 13. Colour distribution for the globular clusters in NGC 7332 after subtraction of the estimated contamination from background galaxies. There is tentative evidence for bimodality in the B–I distribution from KMM statistics. Also shown is the colour distribution of Galatic globular clusters (hatched histograms). The blue peak lies close to the Milky Way distribution (which is dominated by halo globular clusters)

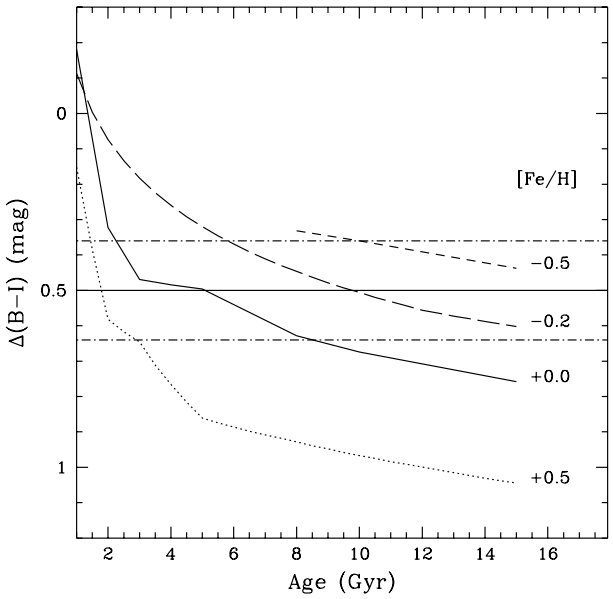

Figure 14. Colour difference versus age diagram for NGC 7332 globular clusters using the Worthey (1994) models. Each curve corresponds to a different metallicity marked on the right of the curve. $\Delta(B-I)$ is defined as the colour difference between the red and the blue (assumed to be 15 Gyr old and metal–poor [Fe/H] $= -1.5$) GC subpopulations. The line corresponds to the measured colour difference in the globular cluster peaks (i.e. $\Delta(B-I) = 0.50 \pm 0.14$).

lation is heavily contaminated by background galaxies). The KMM test indicates roughly equal numbers in each subpopulation. The blue subpopulation has colours consistent with being very old (age $\sim$ 15 Gyrs) and metal–poor ([Fe/H] $\sim$ –1.5). The mean colour difference in the two subpopulations is compared to stellar population models. Although both galaxies have undergone a recent merger, we argue that this event has had little effect on the GC systems. If globular clusters formed in a multi–phase collapse or via accretion, the red ones are required to be metal–poor ([Fe/H] $\sim$ –0.5). The key to discriminating between the models is to determine the age and/or metallicity of individual globular clusters with high S/N spectroscopy.

8 ACKNOWLEDGEMENTS

We thank Soeren Larsen for useful comments and suggestions. We also thank the referee Bill Harris for his insightful comments. Part of this research was funded by NATO Collaborative Research grant CRG 971552 and NSF grant AST 9900732. The data presented herein were obtained at the W.M. Keck Observatory, which is operated as a scientific partnership among the California Institute of Technology, the University of California and the National Aeronautics and Space Administration. The Observatory was made possible by the generous financial support of the W.M. Keck Foundation. This research has made use of the NASA/IPAC Extragalactic Database (NED), which is operated by the Jet Propulsion Laboratory, Caltech, under contract with the National Aeronautics and Space Administration.

REFERENCES

Ashman, K. A., Bird, C. M., Zepf, S. E., 1994, AJ, 108, 2348
Ashman, K. M., Zepf S. E., 1992, ApJ, 384, 50
Bahcall, J. N., Soneira, R. M., 1980, ApJS, 44, 73
Bertin, E., Arnouts, S., 1996, A&AS, 117, 393
Braatz, J. A., Wilson, A. S., Henkel, C., 1994, ApJ, 437, L99
Brown, R. J. N., Forbes D. A., Kissler-Patig M., Brodie J., 2000, MNRAS, 317, 406
Cote, P., Marzke, R. O., West, M. J., 1998, ApJ, 501, 554
Forbes, D.A., Sparks, W., Macchetto, F.D., 1990, In *Paired and Interacting Galaxies*, p 431, ed J. Sulentic, W. Keel, C. Telesco, NASA.
Forbes, D. A., Ponman, T. J., Brown, R. J. N., 1998, ApJ, 508, L43
Forbes, D. A., Brodie, J. P., Grillmair, C. J., 1997, AJ, 113, 1652
Forbes, D. A., Grillmair, C. J., Williger, G. M., Elson, R. A. W., Brodie, J. P., 1998, MNRAS, 293, 325
Fosbury, R.A.E., Melbold, U., Goss, W.M., Dopita, M.A., 1978, MNRAS, 183, 549

Georgakakis, A., Forbes, D. A., Brodie, J. P., 2000, MNRAS, in press
Geisler, D., Lee, M. G., Kim, E., 1996, AJ, 111, 1529
Harris, W. E., 1991, ARA&A, 29, 543
Harris, W. E., Hanes, D. A., 1985, ApJ, 291, 147
Landolt, A. U., 1992, PASP, 104, 336
Lilly, S. J., Cowie, L. L., Gardner, J. P., 1991, ApJ, 369, 79
Oke, J. B., Cohen, J. G., Carr, M., Cromer, J., Dingizian, A., Harris, F., H. Labrecque, S., Lucinio, R., Schaal, W., Epps, H., Miller, J., 1995, PASP, 107, 375
Plana, H., Boulesteix, J., 1996, A&A, 307, 391
Prugniel, P., Simien, F., 1996, A&A, 309, 749
Puzia, T. H., Kissler–Patig, M., Brodie, J. P., Huchra, J. P., 1999, AJ, 118, 2734
Schlegel, D. J., Finkbeiner, D. P., Davis, M., 1998, ApJ, 500, 525
Schweizer, F., 1987, in Nearly Normal Galaxies, ed. S. Faber (Springer: New York), 18
Schweizer, F., Seitzer, P., 1992, AJ, 104, 1039
Terlevich, A. I., Forbes, D. A., 2000, MNRAS, submitted
van Gorkom, J. H., *et al.* 1986, AJ, 91, 791
Worthey, G., 1994, ApJS, 95, 107
Whitmore, B. C., Miller, B. W., Schweizer, F., Fall, S. M., 1997, AJ, 114. 1797